Dipole (hyper)polarizabilities of neutral silver clusters*

Francisco E Jorge[1,2] and Luiz G M de Macedo[3]

[1] Departamento de Física, Universidade Federal do Espírito Santo, 29060-900 Vitória, Brazil
[2] Unidade Acadêmica de Física, Universidade Federal de Campina Grande, 58429-900 Campina Grande, Brazil
[3] Faculdade de Biotecnologia, ICB, Universidade Federal do Pará, 66075-110 Belém, Brazil

(Received 6 June 2016; revised manuscript received 16 August 2016; published online 25 October 2016)

At the Douglas–Kroll–Hess (DKH) level, the B3PW91 functional along with the all-electron relativistic basis sets of valence triple and quadruple zeta qualities are used to determine the structure, stability, and electronic properties of the small silver clusters (Ag_n, $n \leqslant 7$). The results presented in this study are in good agreement with the experimental data and theoretical values obtained at a higher level of theory from the literature. Static polarizability and hyperpolarizability are also reported. It is verified that the mean dipole polarizability per atom exhibits an odd-even oscillation and that the polarizability anisotropy is directly related to the cluster shape. In this article, the first study of hyperpolarizabilities of small silver clusters is presented. Except for the monomer, the second hyperpolarizabilities of the silver clusters are significantly larger than those of the copper clusters.

Keywords: B3PW91 functional, all-electron basis sets, non-relativistic and DKH2 calculations, silver clusters, dipole (hyper)polarizabilities

PACS: 31.15.aj, 31.15.eg, 36.40.–c **DOI:** 10.1088/1674-1056/25/12/123102

1. Introduction

Atomic clusters are considered to be the precursors of bulk material. They represent the transition from the molecular to the solid state physics. Metal clusters have played an important role in cluster physics.[1] They have received the attention of various researchers for their uncommon characteristics, properties, and promising technological applications.[2] For more than thirty years,[3] the properties of metal clusters have been the subject of theoretical[4–13] and experimental[14–21] investigations. Among the properties of metal clusters, the optical properties, which result from the interaction between light and matter, have been extensively studied in the literature.[22]

In this area, the noble-metals Cu, Ag, and Au [electronic configuration: $nd^{10}(n+1)s^1$, $n = 3$, 4, and 5, respectively] have aroused a great deal of interest because they have industrial applications and also because the strong hybridization between their s and d valence orbitals in clusters makes the study of these systems a challenge, i.e., the complexity to describe the electronic states of clusters of noble-metals that lie between the alkali metals and the transition metals.[23–25]

Structural and electronic properties of small silver clusters have received particular attention due to a number of reasons: first, their importance in theoretical and experimental basic researches, in photographic[26] and in catalytic processes,[27] and also the usage in new electronic materials;[28] second, the structures of Ag_3, Ag_4, Ag_5, and Ag_7 are well established in the literature, which have C_{2v}, D_{2h}, C_{2v}, and D_{5h} symmetries (see Ref. [29] and the references therein), respectively.

The static polarizability is a physical observable characteristic that has been used successfully for the understanding of the electronic properties of clusters, since it is sensitive to the delocalization of valence electrons, structure, and shape. In fact, the polarizability is associated with the distortion of the electronic charge distribution due to the application of an external electric field. Furthermore, it is known that there is a relationship between the static dipole polarizability and the shell electronic structure. For example, the static polarizabilities of the noble-metal clusters are lower than those of the alkali metals (see Refs. [30]–[32] and the references therein) because they present a spherical shell structure.

Unlike the static polarizability, the articles reported in the literature about static second hyperpolarizability of metal clusters are scarce and, certainly, it deserves more attention. This point and others for the small silver clusters will be investigated in this work.

It is not easy to compute properties of silver clusters since the computational cost increases quickly with cluster size and also because both the relativistic and electronic correlation contributions must be considered. Effective core potential (ECP) methods have been used to minimize this problem. In this approach, only the valence electrons are taken into account, then, the computational effort is significantly reduced. An alternative to relativistic ECP methods is to employ the density functional theory (DFT) along with a high-quality all-electron basis set at the Douglas–Kroll–Hess (DKH)[33–35]

*Project supported by CNPq, CAPES, and FAPES (Brazilian Agencies).
†Corresponding author. E-mail: Jorge@cce.ufes.br
© 2016 Chinese Physical Society and IOP Publishing Ltd

level. The accuracy that can be achieved with the latter theoretical model on electronic structure calculations of silver clusters has not received due attention in the literature. So, it will be another goal of the present study. It is important to mention here that the DKH approach considers the most part of the scalar relativistic effects.

In this work, the Becke three-parameter for exchange and Perdew–Wang's for correlation (B3PW91)[36,37] hybrid functional in conjunction with the all-electron segmented relativistic basis sets of valence triple and quadruple zeta qualities plus polarization functions (TZP and QZP–DKH)[38,39] for the Ag element are used to evaluate the bond length and the binding energy, ionization potential, electron affinity, and highest occupied molecular orbital (HOMO)–lowest unoccupied molecular orbital (LUMO) gap, respectively, of the ground states of neutral silver clusters (Ag_n, $n \leqslant 7$). The results are compared with experimental and/or theoretical data available in the literature. From the optimized geometries, the static (hyper)polarizabilities are also computed using the non-relativistic augmented QZP (AQZP)[40] basis set. It is the first time that the second hyperpolarizabilities of small silver clusters have been reported.

2. Computational details

All calculations are carried out with the Gaussian 09 program.[41] The TZP–DKH and QZP–DKH basis sets are used with the second-order DKH (DKH2) Hamiltonian, while the AQZP set is used with the non-relativistic Hamiltonian. These sets can be found in different formats at the website https://bse.pnl.gov/bse/portal/.

Initially, the silver cluster equilibrium geometries are determined at the DKH2–B3PW91/TZP–DKH level of theory. Next, from the optimized geometries, the larger QZP–DKH set is used to calculate the binding energies, ionization potentials, electron affinities, and HOMO–LUMO gaps.

The ionization potential (IP), electron affinity (EA), and binding energy (BE), or total atomization energy, are calculated from the following equations

$$\mathrm{IP} = E(N-1) - E(N), \tag{1}$$

$$EA = E(N) - E(N+1), \tag{2}$$

and

$$BE = nE_{\mathrm{Ag}} - E_{\mathrm{Ag}n}, \tag{3}$$

where $E(N-1)$, $E(N)$, and $E(N+1)$ are the energies of clusters containing $(N-1)$, N, and $(N+1)$ electrons, respectively, whereas the mean dipole polarizability, polarizability anisotropy, and second hyperpolarizability can be obtained from the following equations:

$$\bar{\alpha} = \frac{(\alpha_{zz} + \alpha_{xx} + \alpha_{yy})}{3}, \tag{4}$$

$$\Delta\alpha = \left(\frac{1}{2}\right)^{1/2} [(\alpha_{xx} - \alpha_{yy})^2 + (\alpha_{yy} - \alpha_{zz})^2 + (\alpha_{zz} - \alpha_{xx})^2]^{1/2}, \tag{5}$$

$$\bar{\gamma} = \left(\frac{1}{5}\right)(\gamma_{xxxx} + \gamma_{yyyy} + \gamma_{zzzz} + 2\gamma_{xxyy} + 2\gamma_{yyzz} + 2\gamma_{zzxx}). \tag{6}$$

3. Results and discussion

It is known that the ionization potential and electron affinity are very sensitive to the functional employed in the calculations. With this in mind, De Proft and Geerlings[42] carried out extensive investigations about the performances of many different density functional theory (DFT) methods in the computations of these properties for some atomic and molecular systems. Good results are obtained with hybrid functionals. In addition, it should be mentioned here that the B3PW91 hybrid functional has been successfully applied to the study of electronic structures of metal clusters by Jaque and Toro-Labbé[43,44] and by us.[32] In view of this information, this functional seems to be a suitable choice.

3.1. Structure

As mentioned before, the ground state geometric structures of the small silver clusters (Ag_n, $n \leqslant 7$) are among the most well known of the literature. The DKH2–B3PW91/TZP–DKH optimized bond lengths are displayed in Table 1 and the corresponding equilibrium geometries are shown in Fig. 1. From this figure, one can see that the structures from the tetramer until the hexamer and the heptamer have planar and three-dimensional (3D) structures, respectively. It should be noted that the copper clusters present similar behaviors.[32]

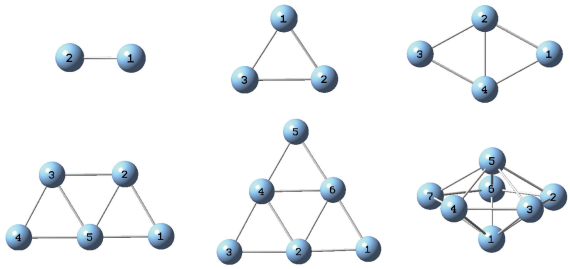


Fig. 1. (color online) Ground state structures of neutral silver clusters, Ag_n ($n = 2$–7).

Among the silver clusters, the dimer and the trimer are the most studied theoretically and experimentally.

For the ground state of the dimer, our calculation gives a bond length of 2.535 Å, which is in excellent agreement with the experimental value of 2.531 Å.[45] Our result also compares well with one (2.52 Å)[4] obtained at a higher level of theory (coupled-cluster with single and double (CCSD) excitations). In Ref. [46], twenty-three DFT methods were used to determine the dimer bond length, but, all of them[46] overestimate the experimental value. In contrast, the B3PW91 functional has been applied successfully to metal cluster propriety

calculations (see Ref. [32] and the references therein). The DKH2–B3PW91/TZP–DKH (205.2 cm^{-1}) and CCSD/11e-RECP-(5s3p2d) (199.3 cm^{-1})[4] harmonic vibrational frequencies overestimate the experimental value (192 cm^{-1})[46] by 6.8% and 3.8%, respectively.

For the trimer, there is strong experimental evidence[47,48] that is an obtuse triangle, but no information about any experimental bond length or bond angle was previously reported. For the large angle and short bond lengths, calculations give values that vary from 63° to 84° and from 2.58 Å to 2.76 Å, being the best estimates close to 68° and 2.68 Å (see Ref. [49] and the references therein), respectively. They are in good and satisfactory accordance with the results found in this work (67° and 2.600 Å).

In turn, Table 1 shows that for all silver clusters, the CCSD/11e–RECP-(5s3p2d) bond lengths agree very well with the B3PW91/TZP–DKH ones, and that, except for a few cases, the difference between corresponding values does not exceed 0.02 Å. We believe that it is the first time that such an accuracy has been achieved with DFT. The optimized bond lengths of the copper clusters[32] obtained at the same level of theory used in this study are systematically smaller than those of the silver clusters about 0.3 Å.

From Table 1, one can verify that the DKH2–B3PW91/TZP–DKH average Ag–Ag bond lengths ($\langle r_{Ag-Ag} \rangle$) for the clusters from Ag_2 to Ag_7 are 2.535, 2.687, 2.675, 2.681, 2.674, and 2.748 Å, respectively. The variation of $\langle r_{Ag-Ag} \rangle$ with n shows clearly structural transitions occurring from 1D (one-dimensional) to 2D (two-dimensional) and from 2D to 3D (three-dimensional). We can also note that $\langle r_{Ag-Ag} \rangle$ increases with the cluster size and it seems to converge to the experimental bulk distance of 2.89 Å. In principle, to achieve the latter value, it will be necessary to take into account larger clusters. However, considering the fact that for $7 \leqslant n \leqslant 12$ an average bond length of 2.74 Å was estimated by Fournier[29] using the VWN exchange–correlation functional, we believe that a very large number of atoms are required to reproduce the bulk distance.

Table 1. Optimized bond lengths r_{ij} (see Fig. 1) for Ag_n clusters. The symmetries are given in parentheses. All values are in unit Å.

Cluster	EOM–CCSD/11e–RECP-(6s5p5d/5s3p2d)[a]	DKH2–B3PW91/TZP–DKH[b]
Ag_2 ($D_{\infty h}$)[c]	$r_{12} = 2.52$	$r_{12} = 2.535$
Ag_3 (C_{2v})	$r_{12} = 2.58$; $r_{23} = 2.88$	$r_{12} = 2.600$; $r_{23} = 2.860$
Ag_4 (D_{2h})	$r_{12} = 2.68$; $r_{24} = 2.58$	$r_{12} = 2.696$; $r_{24} = 2.591$
Ag_5 (C_{2v})	$r_{15} = 2.59$; $r_{12} = 2.62$; $r_{23} = 2.65$; $r_{52} = 2.70$	$r_{15} = 2.649$; $r_{12} = 2.669$; $r_{23} = 2.714$; $r_{52} = 2.708$
Ag_6 (D_{3h})	$r_{24} = 2.69$; $r_{12} = 2.57$	$r_{24} = 2.719$; $r_{12} = 2.651$
Ag_7 (D_{5h})	$r_{23} = 2.75$; $r_{12} = 2.74$	$r_{23} = 2.756$; $r_{12} = 2.744$

[a]From Refs. [4] and [5]. [b]This work. All-electron basis set from Ref. [38]. [c]Experimental value 2.531 Å.[45]

3.2. Binding energy

From the optimized structures, the ground state BEs of all silver clusters are computed at the DKH2–B3PW91/QZP–DKH level. These results and the EOM–CCSD/11e–RECP-(5s3p2d) ones[4] are listed in Table 2.

For the dimer and trimer, the experimental BEs are, respectively, 1.66 eV[45] and 2.61 eV.[48] Our results (1.57 eV and 2.32 eV) are underestimated. The opposite scenario occurs with the EOM–CCSD/11e–RECP-(5s3p2d) ones (1.84 eV and 2.94 eV).[4]

From Table 2, one can note that at any level of theory, the BE and the BE per atom (BE/n) increase with the number of atoms in the cluster. For Ag_4–Ag_7, the DKH2–B3PW91/QZP–DKH binding energies per atom are exactly 0.30 eV smaller than the corresponding ones calculated for the copper clusters[32] using the same level of theory. For Ag_7, our BE per atom is 1.44 eV, while the experimental bulk cohesive energy is 2.96 eV. Once again, larger clusters must be considered to obtain at least a reasonable approximation of the experimental value.

Table 2. Binding energies (BEs) and binding energies per atom (BE/n) of the fully optimized structures of silver clusters Ag_n. All values are in unit eV.

Cluster	11e–RECP-(6s5p5d/5s3p2d)[a]		QZP–DKH[b]	
	BE	BE/n	BE	BE/n
Ag_2	1.84	0.92	1.57	0.785
Ag_3	2.94	0.98	2.32	0.773
Ag_4	5.32	1.33	4.15	1.04
Ag_5	7.45	1.49	5.70	1.14
Ag_6	10.32	1.72	7.83	1.31
Ag_7	11.55	1.65	10.07	1.44

[a]EOM–CCSD results.[4,5] [b]This work (DKH2–B3PW91). All-electron basis set from Ref. [39].

3.3. Ionization potential and electron affinity

The theoretical vertical ionization potentials and electron affinities of the ground states for Ag_n ($n \leqslant 7$) clusters, and experimental data[14–17,51] as well are given in Table 3. From the IP and EA results, characteristic oscillations can be observed. For the ionization potential, the even- and odd-numbered clusters have the maximum and minimum values, respectively, whereas for the electron affinity, the opposite scenario occurs.

Table 3. Vertical ionization potentials (IPs) and electron affinities (EAs) of the fully optimized structures of silver clusters Ag_n. All values are in unit eV.

Cluster	(633321/53211*/531+)[a]		QZP-DKH[b]	AQZP-DKH[c]	Experimental	
	IP	EA	IP	EA	IP[d]	EA[e]
Ag	7.461[f]	1.254[f]	7.770	1.134	7.576[g]	1.302[g]
Ag_2	7.73	–	7.733	0.918	7.60	1.028
Ag_3	5.67	–	5.756	0.984	6.20	2.380
Ag_4	6.54	–	6.433	1.672	6.65	1.600
Ag_5	6.33	–	6.124	2.032	6.35	2.100
Ag_6	7.22	–	7.034	1.373	7.15	2.000
Ag_7	6.36	–	5.862	1.860	6.40	2.400

[a]PW non-relativistic calculations.[7] All-electron basis set. [b]This work (DKH2–B3PW91). All-electron basis set from Ref. [39]. [c]This work (DKH2–B3PW91). All-electron basis set from Refs. [39] and [40]. [d]From Refs. [14] and [15]. [e]From Refs. [16] and [17]. [f]DK–CCSD(T) calculations.[52] NpPolMe + (3s3p1d1f) all-electron basis set. [g]From Ref. [51].

It is known that silver clusters containing an even (odd) number of atoms have a closed (open) shell. It is more difficult to remove an electron in a doubly occupied HOMO than in a simply occupied HOMO. That is the reason for the even-numbered cluster displaying larger IP. In contrast, it is easier to acquire an electron in an open-shell HOMO than in an LUMO of the closed-shell system then, the maximum EA values must occur for odd-numbered clusters.

For Ag, the DKH2–B3PW91/QZP–DKH vertical IP of 7.770 eV compares well with the experimental[51] and DK–CCSD(T)/NpPolMe + (3s3p1d1f)[52] values of 7.576 eV and 7.461 eV, respectively. Except for Ag_7, where our result (5.862 eV) is underestimated and the PW/(633321/53211*/531+) one (6.36 eV)[7] is closer to the experimental vertical IP (6.40 eV),[15] the other DFT results displayed in Table 3 are in good agreement with each other. For Ag_3, the DKH2–B3PW91/QZP–DKH approach gives 5.756 eV. In the literature, we find two experimental measurements of the vertical IP for the trimer: 5.6 eV[19] and 6.20 eV (upper bound).[15] For Ag_2, Ag_4, Ag_5, and Ag_6, the accordance between theory and experiment is good (cf. Table 3). The IPs of the copper clusters[32] exceed those of the silver clusters by 0.30 eV, similarly for the binding energies.

Now, considering the EA, one can note that our results are systematically lower than the experimental ones and, with the exception of Ag_3, that they have the same pattern as the experimental data. The vertical EA results are scarce in the literature for silver clusters, and for this reason no other theoretical values are included in Table 3.

3.4. (Hyper)polarizabilities

The static polarizability is one of the most important electronic properties of clusters, because it is sensitive to the number of electrons, structure, and shape of the system.

From the DKH2–B3PW91/TZP–DKH optimized geometries (see Table 1), non-relativistic calculations of the mean dipole polarizability ($\bar{\alpha}$), mean dipole polarizability per atom ($\bar{\alpha}/n$), polarizability anisotropy ($\Delta\alpha$), and the second hyperpolarizability ($\bar{\gamma}$) of Ag_n ($n \leqslant 7$) are carried out at the B3PW91/AQZP level. PW/(633321/53211*/531+) dipole polarizability results[7] and our findings are displayed in Table 4.

Table 4 shows that at any level of theory, the mean dipole polarizabilities increase monotonically according to the sequence from Ag to Ag_7, i.e., the so expected proportionality to the total number of electrons is confirmed. A similar behavior is observed for the copper clusters[32]. We also note that the $\bar{\alpha}$ values of the silver clusters are larger than those evaluated for the analogous copper clusters (see Table 4 of Ref. [32]). This difference originates from the additional screening due to 3d4s4p electrons, which takes place on silver clusters. For the silver clusters from Ag to Ag_3, the mean dipole polarizabilities show to be sensitive to the used theoretical procedure. Our values are larger than those computed in Ref. [7]. However, from Ag_4 both the models give very similar results (cf. Table 4). The polarizabilities[6] calculated from the PBE functional add credence to these findings. For the larger silver clusters, it looks as if the $\bar{\alpha}$ values are less dependent on the exchange–correlation functional and basis set used.

For $n \leqslant 6$, the calculated B3PW91/AQZP polarizabilities per atom present odd–even oscillation. It is a characteristic of clusters of atoms with an odd number of electrons like Cu, Ag, and Au and the alkali metals. This oscillation is associated with the odd–even oscillation of the HOMO–LUMO gaps calculated at the DKH2–B3PW91/TZP–DKH level of theory. From Ag to Ag_7 the HOMO–LUMO gaps obtained in this work are, respectively, 2.26, 3.17, 1.17, 1.84, 1.43, 3.19, and 1.35 eV. An increase of the HOMO–LUMO gap of a given cluster is directly related to its chemical stabilization, which in turn conduces to the decrease of its static polarizability. Our results show clearly that the clusters with small HOMO–LUMO gaps have larger polarizabilities per atom. Therefore, the maximum static polarizabilities and HOMO-LUMO gaps happen to the odd and even clusters, respectively. The odd–even oscillation finishes at $n = 7$ because there is a transition

from the 2D to the compact 3D structure, consequently, the polarizability and HOMO–LUMO gap of Ag_7 are reduced when compared with the corresponding Ag_6 values. In this case, the structure symmetry is more important than the HOMO–LUMO gap. For the polarizabilities per atom and HOMO–LUMO gaps, similar trends are observed for the Cu_n ($n \leqslant 8$) clusters.[32] We also note that the $\bar{\alpha}/n$ values for Ag and Ag_3 are both 15 a.u. larger than the corresponding values obtained for Cu and Cu_3, and that this difference decreases to 10 a.u. for $n = 2$ and from $n \geqslant 4$.

Table 4. Values of static electric mean dipole polarizability ($\bar{\alpha}$), mean dipole polarizability per atom ($\bar{\alpha}/n$), polarizability anisotropy ($\Delta\alpha$), and the second hyperpolarizability ($\bar{\gamma}$). All values are in unit a.u. (atomic unit).

Cluster	(633321/53211*/531+)[a]			AQZP[b]			
	$\bar{\alpha}$	$\bar{\alpha}/n$	$\Delta\alpha$	$\bar{\alpha}$	$\bar{\alpha}/n$	$\Delta\alpha$	$10^{-3}\times\bar{\gamma}$
Ag	46.23	46.23	0.00	61.51	61.51	0.00	12.25[c]
Ag_2	92.86	46.43	85.43	102.88	51.44	62.89	150.54[d]
Ag_3	159.13	53.04	145.97	187.85	62.62	164.28	134.52
Ag_4	193.00	48.25	211.36	193.27	48.32	173.49	457.79
Ag_5	248.00	49.60	227.42	247.09	49.42	192.31	482.97
Ag_6	289.50	48.25	230.39	279.14	46.52	193.34	464.12
Ag_7	305.63	43.66	97.78	308.18	44.03	87.14	563.13

[a]PW non-relativistic calculations.[7] All-electron basis set. [b]This work (B3PW91). All-electron basis sets from Ref. [40]. [c]Equation (6) reduces to $\bar{\gamma} = 3/5(\gamma_{zzzz} + 2\gamma_{xxzz})$. [d]Equation (6) reduces to $\bar{\gamma} = (3\gamma_{zzzz} + 8\gamma_{xxxx} + 12\gamma_{xxzz})/15$.

For Ag, the experimental mean dipole polarizability of 53.31 a.u. is underestimated and overestimated by the non-relativistic PW/(633321/53211*/531+) and B3PW91/AQZP calculations (cf. Table 4), respectively. Kellö and Sadlej[53] in their study of some neutral transition metals verified that the mean dipole polarizabilities decreased when relativistic effects were included in the calculations. For example, for Ag, the non-relativistic $\bar{\alpha}$ value of 37.60 a.u. was diminished to 30.02 a.u.[53] by using the DK no-pair formalism. So, it is expected that the inclusion of the relativistic effect certainly reduces our result of 61.51 a.u. and moves it closer to the experimental value.

Except for Ag_3, the polarizability anisotropies obtained in this work are at least 10% smaller than those reported by Pereiro and Baldomir.[7] Unlike the mean dipole polarizability, the polarizability anisotropy displays a strong dependence obtained with using the theoretical model. From Table 4, one can note that the B3PW91/AQZP polarizability anisotropies increase in the order from Ag_2 to Ag_6 but decreases for Ag_7, i.e., there is a maximum value at the hexamer. These results along with the topologies of the silver clusters show clearly that the $\Delta\alpha$ value is related to the cluster structure. At the planar clusters, they increase with n increasing. In contrast, when the cluster structure becomes compact the polarizability anisotropy decreases. It is the case of the heptamer. It should be noted that the result for Ag_7 is not so different from that obtained for Ag_2 (open structure). Similar findings were reported by Jorge *et al.*[32] in their study of polarizability anisotropies of copper clusters.

The B3PW91/AQZP second hyperpolarizabilities for the silver clusters are presented in Table 4. Just as it occurs for the copper clusters,[32] the hyperpolarizability values for the silver clusters increase substantially from $n = 4$. To the best of our knowledge, it is the first time that the second hyperpolarizabilities of small silver clusters have been published in the literature. So, a comparison will be done with the B3PW91/AQZP results obtained recently[32] for the copper clusters. With the exception of Ag, the hyperpolarizabilities of the silver clusters are significantly higher than the corresponding ones calculated for the copper clusters, and the difference reaches 198.10 a.u. for Ag_7. The results reported in this work are certainly useful for further calculations on the second hyperpolarizability of silver clusters.

4. Conclusions

In this paper, the bond length, binding energy, ionization potential, electron affinity, and HOMO–LUMO gap of small silver clusters (Ag_n, $n \leqslant 7$) are studied at the DKH2–B3PW91/*X*ZP–DKH (X = T or Q) level of theory. Non-relativistic calculations of static dipole (hyper)polarizabilities are also carried out. The general trend that we can extract from our results is that the even-numbered silver clusters are more stable (or less reactive) than the odd-numbered ones.

The following specific conclusions can be drawn from our results.

(i) For all studied silver clusters, the DKH2–B3PW91/TZP–DKH bond lengths agree very well with those obtained with a higher level of theory [EOM–CCSD/11e–RECP-(6s5p5d/5s3p2d)]. For the dimer, the difference between the DKH2–B3PW91/TZP–DKH and experimental results is only 0.004 Å.

(ii) The binding energy per atom increases with cluster size.

(iii) The ionization potential and electron affinity present odd–even oscillations, which are in agreement with those from the chemical insight. Except for Ag_7, the accordance between our results and the experimental ionization potentials is good. In contrast, the electron affinities are underestimated.

(iv) The HOMO–LUMO gaps also show an odd–even oscillating feature. As expected, the oscillation of the mean dipole polarizabilities per atom is the inverse of that of the HOMO–LUMO gaps.

(v) At the same level of theory, we verify that the results obtained for the copper clusters[32] display similar trends to

those for the silver clusters. However, as the electronic structures of copper cluster are more compact than those of the silver clusters, it can have a great effect on the property magnitudes of these clusters.

Finally, we note for the silver clusters that the polarizability anisotropy is more sensitive to the theoretical procedure used than the mean dipole polarizability and that the second hyperpolarizability values increase considerably from $n \geqslant 4$. As the hyperpolarizability results reported in this work are unique, they can be helpful for further DFT and/or *ab initio* calculations.

References

[1] De Heer W A 1993 *Rev. Mod. Phys.* **65** 611
[2] Jellinek J 1999 *Theory of Atomic and Molecular Clusters* (Berlin: Springer)
[3] Ekardt W 1999 *Metal Clusters* (Chichester: Wiley)
[4] Koutecky V B, Pittner J, Boiron M and Fantucci P 1999 *J. Chem. Phys.* **110** 3876
[5] Koutecky V B, Veyret V and Mitric R 2001 *J. Chem. Phys.* **115** 10450
[6] Idrobo J C, Öğüt S and Jellinek J 2005 *Phys Rev B* **72** 085445
[7] Pereiro M and Baldomir D 2007 *Phys. Rev. A* **75** 033202
[8] Lu Z H and Cao J X 2008 *Chin. Phys. B* **17** 3336
[9] Li W Y and Chen F Y 2014 *Chin. Phys. B* **23** 117103
[10] Zhang J F, Zhang M, Zhao Y W, Zhang H Y, Zhao L N and Luo Y H 2015 *L Chin. Phys. B* **24** 067101
[11] Chang Y, Li W and Jiang Y 2012 *Phys. Lett. A* **376** 2314
[12] Lv J, Zhang J Y, Liang R R and Wu H S 2016 *Chin. Phys. B* **25** 063103
[13] Guo P, Zheng J M, Zhao P, Zheng L L and Ren Z Y 2010 *Chin. Phys. B* **19** 083601
[14] Rabin I, Jackschath C and Schulze W 1991 *Z. Phys. D: At. Mol. Clusters* **19** 153
[15] Jackschath C, Rabin I and Schulze W 1992 *Z. Phys. D: At. Mol. Clusters* **22** 517
[16] Spasov V A, Lee T H, Maberry J P and Ervin K M 1999 *J. Chem. Phys.* **110** 5208
[17] Shi Y, Spasov V A and Ervin K M 1999 *J. Chem. Phys.* **111** 938
[18] Ho J, Erwin K M and Lineberger W C 1990 *J. Chem. Phys.* **93** 6987
[19] Alammeddin G, Hunter J, Cameron D and Kappes M M 1992 *Chem. Phys. Lett.* **192** 122
[20] Handschuh H, Cha C Y, Bechthold P S, Ganteför G and Eberhardt W 1995 *J. Chem. Phys.* **102** 6406
[21] Khan S A, Senapati D, Senapati T, Bonifassi P, Fan Z, Singh A K, Neeley A, Hill G and Ray P C 2011 *Chem. Phys. Lett.* **512** 92
[22] Kreibig U and Vollmer M 1995 *Optical Properties of Metal Clusters* (Berlin: Springer)
[23] Felix C, Sieber C, Harbich W, Buttet J, Rabin I, Schulze W and Ertl G 1999 *Chem. Phys. Lett.* **313** 105
[24] Rabin I, Schulze W, Ertl G, Felix C, Sieber C, Harbich W and Buttet J 2000 *Chem. Phys. Lett.* **320** 59
[25] Felix C, Sieber C, Harbich W, Buttet J, Rabin I, Schulze W and Ertl G 2001 *Phys. Rev. Lett.* **86** 2992
[26] Mostafavi M, Marignier J L, Amblard J and Belloni J 1989 *Z. Phys. D: At. Mol. Clusters* **12** 31
[27] Tani T 1989 *Phys. Today* **42** 36
[28] Kim S H, Medeiros-Ribeiro G, Ohlberg D A A, Williams R S and Heath J R 1999 *J. Phys. Chem.* **103** 10341
[29] Fournier R 2001 *J. Chem. Phys.* **115** 2165
[30] Pan X D, Gai Z G and Li G P 2008 *Chin. Phys. B* **17** 3329
[31] De Souza F A L and Jorge F E 2013 *J. Braz. Chem. Soc.* **24** 1357
[32] Jorge F E, Ferreira I B, Soprani D D and Gomes T 2016 *J. Braz. Chem. Soc.* **27** 127
[33] Douglas M, Kroll N M 1974 *Ann. Phys.* **82** 89
[34] Hess B A 1985 *Phys. Rev. A: At. Mol. Opt. Phys.* **32** 756
[35] Hess B A 1986 *Phys. Rev. A: At. Mol. Opt. Phys.* **33** 3742
[36] Becke A D 1993 *J. Chem. Phys.* **98** 5648
[37] Perdew J P, Wang W R 1992 *Phys. Rev. B: Condens. Matter Mater. Phys.* **45** 13244
[38] Campos C T and Jorge F E 2013 *Mol. Phys.* **111** 167
[39] Ceolin G A, de Berrêdo R C and Jorge F E 2013 *Theor. Chem. Acc.* **132** 1339
[40] Martins L S C, de Souza F A L, Ceolin G A, Jorge F E, de Berrêdo R C and Campos C T 2013 *Compt. Theor. Chem.* **1013** 62
[41] Frisch M J, Trucks G W, Schlegel H B, Scuseria G E, Robb M A, Cheeseman J R, Montgomery J A Jr, Vreven T, Kudin K N, Burant J C, Millam J M, Iyengar S S, Tomasi J, Barone V, Mennucci B, Cossi M, Scalmani G, Rega N, Petersson G A, Nakatsuji H, Hada M, Ehara M, Toyota K, Fukuda R, Hasegawa J, Ishida M, Nakajima T, Honda Y, Kitao O, Nakai H, Klene M, Li X, Knox J E, Hratchian H P, Cross J B, Adamo C, Jaramillo J, Gomperts R, Stratmann R E, Yazyev O, Austin A J, Cammi R, Pomelli C, Ochterski J W, Ayala P Y, Morokuma K, Voth G A, Salvador P, Dannenberg J J, Zakrzewski V G, Dapprich S, Daniels A D, Strain M C, Farkas O, Malick D K, Rabuck A D, Raghavachari K, Foresman J B, Ortiz J V, Cui Q, Baboul A G, Clifford S, Cioslowski J, Stefanov B B, Liu G, Liashenko A, Piskorz P, Komaromi I, Martin R L, Fox D J, Keith T, Al-Laham M A, Peng C Y, Nanayakkara A, Challacombe M, Gill P M W, Johnson B, Chen W, Wong M W, Gonzalez C and Pople J A 2003 *Gaussian* 03, Revision A.1 (Pittsburgh: Gaussian, Inc.)
[42] De Proft F and Geerlings P 1997 *J. Chem. Phys.* **106** 3270
[43] Jaque P and Toro-Labbé A 2002 *J. Chem. Phys.* **117** 3208
[44] Jaque P and Toro-Labbé A 2014 *J. Mol. Model.* **20** 2410
[45] Simard B, Hackett P A, James A M and Langridge-Smith P R R 1991 *Chem. Phys. Lett.* **186** 415
[46] Zhao S, Li Z H, Wang W N, Liu Z P, Fan K N, Xie Y and Schaefer III H F 2006 *J. Chem. Phys.* **124** 184102
[47] Wallimann F, Frey H M, Leutwyler S and Riley M 1997 *Z. Phys. D: At. Mol. Clusters* **40** 30
[48] Yoon J, Kim K S and Baeck K K 2000 *J. Chem. Phys.* **112** 9335
[49] Ellis A M, Robles E S J and Miller T A 1993 *Chem. Phys. Lett.* **201** 132
[50] Hilpert K and Gingerich K A 1980 *Ber. Bunsenges. Phys. Chem.* **84** 739
[51] Moore C E 1958 *Natl. Bur. Stand. Circ.* **3** 467
[52] Neogrády P, Kellö V, Urban M, Sadlej A J 1997 *Int. J. Quantum Chem.* **63** 557
[53] Kellö V and Sadlej A J 1996 *Theor. Chim. Acta* **94** 93